Low-pressure and Nascent Yields of Thermalized Criegee Intermediate in Ozonolysis of Ethene

*Lei Yang, Mixtli Campos-Pineda,[a] Jingsong Zhang**

Department of Chemistry

University of California, Riverside

Riverside, CA 92521

USA

[a] Present address: Centre for Research into Atmospheric Chemistry, University College Cork, T12 YN60, Ireland

* Corresponding author. Email: jingsong.zhang@ucr.edu; Tel +1 951 827 4197; Fax: +1 951 827 4713. Also at Air Pollution Research Center, University of California, Riverside, California 92521, United States.

Abstract

The yields of thermalized formaldehyde oxide (CH_2OO, the simplest Criegee intermediate) produced from ozonolysis of ethene at low pressures were measured indirectly using cavity ring-down spectroscopy (CRDS) and chemical titration with an excess amount of sulfur dioxide (SO_2). The method of monitoring the consumption of SO_2 as a scavenger allows better characterization of the CH_2OO at low pressure and short residence time. The yield of thermalized CH_2OO from ethene ozonolysis was found to decrease with decreasing pressure. The nascent yield of thermalized CH_2OO was determined to be 20.1 ± 2.5% by extrapolating the 7-19 Torr measurements to the zero-pressure limit. Kinetic models enable better evaluation and understanding of the different measurement methods of thermalized Criegee intermediates (tCIs). The information on the low-pressure yields from this work serves as a benchmark for theoretical calculations and facilitates a better understanding of the alkene ozonolysis reaction mechanisms.

Table of Contents Graphic

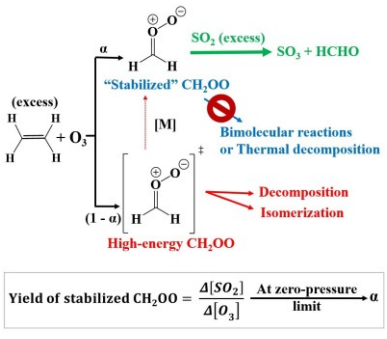

Keywords: ozonolysis, ethene, Criegee intermediate, cavity ringdown spectroscopy

Ozonolysis is an important oxidation pathway of unsaturated volatile organic carbons (VOCs) in the troposphere because of its important role in the production of HO_x (OH and HO_2) and RO_x radicals and the formation of secondary organic aerosol (SOA).[1-3] In the ozonolysis reactions of alkenes, the cycloaddition of ozone (O_3) to the C=C double bonds produce chemically activated primary ozonides (POZ), which then decompose into carbonyls and carbonyl oxides (Criegee intermediates, CIs). After the highly-exothermic decomposition of POZ through the cleavage of the C-C bond and one of the O-O bonds on the five-membered ring, CIs are produced with broad internal energy distributions.[4] CIs have two resonance structures, the biradical and zwitterion structures, and are the most unstable among all their isomers. Therefore, they can readily isomerize into dioxirane via endocyclic addition, or vinyl hydroperoxide via hydrogen shifts, and then decompose into products such as OH radicals. CIs could undergo both unimolecular dissociations and bimolecular reactions. The branching ratio depends on their internal energy compared to the dissociation or isomerization energy barrier. High-energy CIs can decompose rapidly into atmospherically important species such as OH and organic radicals, while thermalized Criegee intermediates (tCIs) have less energy than the unimolecular decomposition barrier. Although historically called stabilized Criegee intermediates, recent experimental studies of tCIs indicate that they are more reactive than initially anticipated, and thus the term "thermalized Criegee intermediates" is used here instead. With a longer lifetime than high-energy CIs, tCIs could take part in bimolecular reactions or thermal decay via tunnelling.[5, 6]

Decades of research efforts have shown the difficulty in direct measurement and characterization of CIs produced from ozonolysis due to their transient lifetimes and low steady-state concentrations. In 2012, photolysis of diiodo-alkane in an excess amount of oxygen was developed to produce stable CIs by Weltz and co-workers[7] and allowed direct detection of tCIs

via photoionization, infrared, ultraviolet, and rotational spectroscopy.[8] Since then, kinetic studies on the unimolecular decomposition rates of tCIs and their bimolecular reactions with atmospheric species have been reported by many research groups.[9-11] Nevertheless, the energy distributions of CIs and yields of tCIs in ozonolysis of alkenes which are relevant to the branching ratio of different reaction pathways of CIs in the troposphere, cannot be studied from the photolysis synthesis method. Instead, the yields of tCIs vs. high-energy CIs produced from ozonolysis of alkenes can only be measured by performing actual ozonolysis reactions. Therefore, several groups have reported using chemical titration to determine the yield of tCIs, as summarized in Table S1 in Supporting Information (SI). With an excess amount of scavenger, which can selectively react with tCIs rapidly before they undergo other bimolecular processes or thermal decomposition, the amount of tCIs can be measured by monitoring either the product of the reaction between tCIs and the scavenger or the depletion of the scavenger. For example, sulfur dioxide (SO_2) has been used to titrate tCIs produced from some short chain alkenes, isoprene, and monoterpenes, and the yields of tCIs were determined by measuring either the production of sulfuric acid (H_2SO_4)[12-15] or carbonyls[16] or depletion of SO_2.[17-19] While various kinds of molecules have also been explored and used as tCI scavengers previously (such as HCHO, HCOOH, CH_3OH, H_2O, CO, and hexafluoroacetone),[20, 21] SO_2 is chosen as the scavenger in this work owing to its fast and selective reactions with tCIs and characterizable UV spectral features.

Many theoretical and experimental works have focused on predicting the energy profile of the ozonolysis reaction of ethene and determining the yield of thermalized CH_2OO, while the reported values vary significantly from each other. At atmospheric pressure, experimental literature values of tCI yield in ozonolysis of ethene range from 35% to 54%.[22] Even though the

atmospheric pressure tCI yields have been determined in many alkene ozonolysis systems, the studies on nascent yields of tCIs are relatively limited. The yield of tCIs has been reported to be pressure-dependent for most acyclic alkenes. The tCIs can either come from the nascent decomposition reaction of POZ or be formed from the collisional stabilization of high-energy CIs or POZ. Therefore, to understand the original energy profile of the reaction, measuring the nascent yield of tCIs near a zero-pressure limit is essential. Moreover, the nascent energy distribution is also of theoretical interest for direct comparison with reaction dynamics calculations. The nascent yield of tCIs has only been reported for a few systems so far, and systematic studies on the nascent yields are still limited, while it is an important benchmark for reaction mechanism calculations. Among the reported nascent tCI yield results, some groups have measured the tCI yields at different pressures ranging from tens of Torr to atmospheric pressure, then extrapolated to the zero-pressure limit to obtain the nascent yield.[14, 21] However, the pressure-dependence of tCIs may not always be in a linear relationship from 0-1000 Torr according to these reports, and the increase of the tCI yield with increasing pressure at the low-pressure end could be faster than at higher pressure, which suggests that the deactivation rate of high-energy CIs to tCIs via collisions with buffer gases is likely to be pressure-dependent. Thus, to accurately measure the nascent yield, the low-pressure region should be focused on.

The method of monitoring H_2SO_4 needs a large amount of water to fully convert SO_3 from the tCI + SO_2 titration reaction and thus does not work well at low pressure and short residence time. In this work, cavity ring-down spectroscopy (CRDS) was utilized in combination with chemical titration with SO_2 to quantify tCIs by monitoring the consumption of SO_2 (Figure S1). The ozonolysis reactions of ethene were carried out under various flow and low-pressure conditions ranging from 7-19 Torr. Reference cross-sections of the species involved, SO_2, O_3, and

formaldehyde (HCHO, mainly produced from the decomposition of POZ as the coproduct of CI), were fitted with their spectral features to obtain the number densities. The nascent yield of the simplest tCI, thermalized formaldehyde oxide (CH_2OO), in ozonolysis of ethene was determined by extrapolation from 7-19 Torr to zero pressure. The present method allows a systematic study of the total nascent yield of tCIs produced from ozonolysis of alkenes.

The experiment was designed using rapid titration of tCIs with SO_2. As shown in Figure 1, UV absorption spectra in the wavelength range from 323.5 nm to 325.2 nm of the mixture of ethene and O_3 provided final O_3 concentrations ($[O_3]_f$) after they were fitted to the spectral features of O_3 and HCHO; then ethene was replaced with the same amount of N_2 and the UV spectra were measured to obtain the initial O_3 concentration ($[O_3]_i$). Similarly, under the same pressure, flow rate, and initial concentrations, the UV spectra of the mixture of ethene, O_3 and SO_2 were measured to obtain the final concentration of SO_2 ($[SO_2]_f$) after being fitted to the spectral features of O_3, HCHO and SO_2, and then the ozonolysis reactants were replaced by N_2 to measure the initial amount of SO_2 ($[SO_2]_i$). The reference cross sections of O_3, SO_2, and HCHO were selected from the database of the MPI-Mainz UV/VIS Spectral Atlas[23] according to the wavelength ranges and spectral resolution and then fitted to our experimental spectra to create our references, which minimized the difference in the measurement sensitivities (especially for HCHO whose rovibronic features could be shifted and affected by different energy distributions).

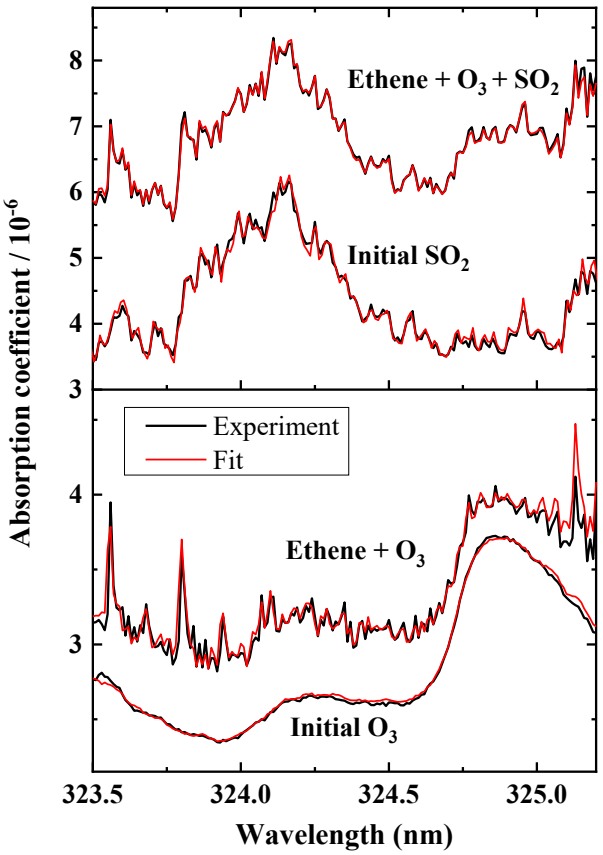

Figure 1. Representative UV absorption spectra (black lines) and corresponding fitting results (red lines) of O_3 and SO_2 from the ozonolysis reaction of ethene (ethene + O_3) and the titration reaction with SO_2 (ethene + O_3 + SO_2). The spectra from the ozonolysis reaction were fitted to the UV spectra features of O_3 and HCHO, while the spectra from the titration reaction were fitted to the spectra features of O_3, HCHO and SO_2 with the broad background contribution from secondary reactions. Concentrations of the reactants and products in this example (unit: molecules cm^{-3}): $[O_3]_i = 2.03\times10^{14}$, [Ethene]i = 2.11×10^{17}, $[O_3]_f = 1.50\times10^{14}$, $[SO_2]_i = 3.44\times10^{14}$, $[SO_2]_f = 3.30\times10^{14}$, $[HCHO]_i$ (in ethene + O_3) = 4.5×10^{14}, $[HCHO]_f$ (in ethene + O_3 + SO_2) = 5.5×10^{14}. The total pressure in this example was 19 Torr, and the residence time inside the flow reactor was about 1.3 seconds. All experiments in this work were carried out at room temperature.

As ethene was about three orders of magnitude in excess to O_3 and it reacts with the OH radical rapidly (with a rate constant $k(C_2H_4 + OH) = 2.8\text{-}4.8\times10^{-12}$ cm^3 $molecule^{-1}$ s^{-1} at 5-19 Torr and 7.8×10^{-12} cm^3 $molecule^{-1}$ s^{-1} at 1 atm), the large excess amount of alkene completely scavenged the highly reactive OH radicals produced in ozonolysis before they reacted with any

other species (including SO_2 in the titration measurements). The excess amount of titrant SO_2 dominated the reactions of tCIs, depleting them with a fast rate constant of 3.7×10^{-11} cm^3 $molecule^{-1}$ s^{-1}. Hence, the amount of consumed SO_2 was equal to the amount of tCIs produced in the ozonolysis reaction. Since the extent of ozonolysis was equal to the amount of consumed O_3 via its reaction with ethene, the yield of tCIs can be determined by the following equation:

$$\text{Yield of tCI} = \frac{\Delta[SO_2]}{\Delta[O_3]} \qquad (1)$$

where the consumed amount of SO_2 is $\Delta[SO_2] = [SO_2]_i - [SO_2]_f$ and the consumed amount of O_3 is $\Delta[O_3] = [O_3]_i - [O_3]_f$.

Equation (1) is validated when the SO_2 concentration is sufficiently high to completely titrate all the thermalized CH_2OO produced from the ozonolysis reaction before tCIs undergo unimolecular reaction or bimolecular reactions with any other species such as ethene, O_3 and HCHO. As CRDS has a limited dynamic range in measurement (typically two orders of magnitude), using too much SO_2 would result in a rapid increase of the ringdown decay rate, which would make the signal too noisy to be reliably measured. In addition, unnecessarily high-concentration SO_2 would promote the formation of secondary products, which could increase the broad background in the absorption spectra. Therefore, to determine the minimum amount of SO_2 needed to effectively consume all the tCIs, a titration curve was obtained by measuring the change in the ratio of consumed SO_2 to consumed O_3 when varying the initial concentration of SO_2 under the same pressure, residence time and initial reactant concentrations. As shown in Figure 2, since O_3 was the limiting reagent in the ozonolysis reaction studied in this work (ethene concentration was about three orders of magnitude higher than O_3), the ratio of initial concentration of SO_2 to O_3 was used as the horizontal axis. The ratio of consumed SO_2 to O_3 would increase when the initial SO_2 was much lower than the initial concentration of O_3 and then

reached a stable value as the initial SO_2 increased. The plateau in the titration curve indicated the maximum consumption of SO_2 and thus the completion of titration of tCIs when the SO_2 concentration was higher than 1.5×10^{14} molecules cm^{-3} (with the initial $[SO_2]/[O_3] > 0.8$). Considering that the consumed O_3 was about 25% of its initial concentration under the current condition and the yield of tCIs in ozonolysis at low pressure is typically lower than 40%, the amount of SO_2 on the plateau was more than ten times higher than the total amount of tCIs. The high concentration of SO_2 used in the tCI measurement experiments (with the initial $[SO_2]/[O_3]$ = 1.1-1.7) and the large rate constant of the SO_2 + tCI (CH_2OO) reaction ($k = 3.7\times10^{-11}$ cm^3 $molecule^{-1}$ s^{-1}) allowed the SO_2 + tCI scavenging reaction to be dominant over all other tCI reaction pathways. This is also supported by the calculated titration trend line from the kinetic modeling of the ethene ozonolysis built for the titration reaction using the Kintecus software package[24] (see Table S3 and Figure S2 in SI for more information). The calculated trend line of $\Delta[SO_2]/\Delta[O_3]$ (Figure 2) agrees well with our measurements except at the very beginning when the SO_2 concentration was not high enough to be dominant and some other pathways of CH_2OO affected the shape of the curve. The error bars in the experimental measurements representing one standard deviation of five repeated measurements are relatively large because of the slow rate constant ($k = 1.55\times10^{-18}$ cm^3 $molecule^{-1}$ s^{-1}) of the reaction between ethene and O_3, which limited the extent of the reaction in the short residence time used in this work (1.1-1.6 seconds). Even though, it was still necessary to keep the residence time short (less than 2 seconds) since a longer reaction time would accumulate secondary products (such as HCOOH, carbonyls, and SOA), which would not only contribute to the broad UV absorption background and reduce the detection sensitivity but also compete with SO_2 to react with CH_2OO according to our experimental observations and modeling calculations.

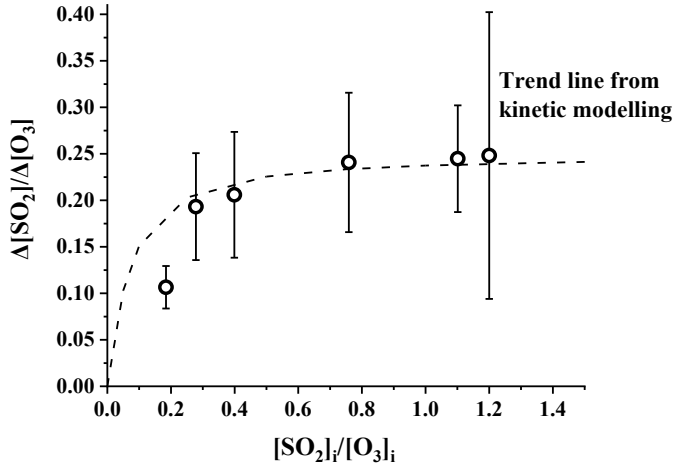

Figure 2. Titration curve by varying the initial SO_2 concentration at a total pressure of 13 Torr showing the change in the consumption of SO_2 in the ethene ozonolysis reaction. The horizontal axis is the ratio of the initial SO_2 concentration and initial O_3 concentration, representing the excess extent of the SO_2 titrant. The initial O_3 concentration was kept at a constant value of $\sim 2 \times 10^{14}$ molecules cm^{-3} throughout the titration curve. The vertical axis is the ratio of the consumed amount of SO_2 and O_3, which reached a maximum of about 25% when the added SO_2 had a sufficiently high concentration to completely titrate all the produced tCIs in ozonolysis of ethene. The trend line was calculated from the kinetic modeling. Error bars represent one standard deviation of repeated measurements at each SO_2 condition.

The measured yield of thermalized CH_2OO produced from ozonolysis of ethene in the pressure range of 7-19 Torr is shown in Figure 3. Special attention was paid to the concentration of SO_2 during the experiments to ensure that the initial $[SO_2]/[O_3]$ ratio was on the plateau of the titration curve and SO_2 could completely titrate all the thermalized CH_2OO at each pressure. The linear fit of the trend shows that the tCI yield decreases with decreasing pressure, and extrapolation to the zero-pressure limit shows the nascent yield of thermalized CH_2OO is 20.1 ± 2.5%. When the pressure was below 10 Torr, the extent of the reaction was relatively small due to the lower initial concentrations and short residence time, resulting in smaller values of $\Delta[O_3]$ and $\Delta[SO_2]$, which increased the error bars at 7 and 8 Torr. The uncertainty of the nascent yield of tCI, 2.5%, was calculated by multiplying the 95% confidence *t*-test value with the standard error of the intercept from the weighted linear fit of the six data points using the least-squares

method (more details are in the description of Table S4 in SI). The previous studies by Hatakeyama et al. determined the yield of tCI in ozonolysis of ethene at 10-1140 Torr by monitoring the H_2SO_4 produced in the titration reaction using SO_2.[13] Their measurements from 10 to 22 Torr (with 3 data points) are plotted and extrapolated in Figure 3 for comparison. The nascent yield obtained from extrapolation of their low-pressure data is 18.2 ± 3.4% at the zero-pressure limit, ~ 2% lower than our measurement but in agreement within the error limits from both studies. Our yields are 3-4% higher than theirs in the 10-22 Torr range. Note that for the titration reaction between CH_2OO and SO_2, although the HCHO and SO_3 formation is the main pathway (68%), alternative channels involving the formation of diradical $CH_2(O\bullet)O\bullet$ (17%) and formylsulfinic acid HC(=O)OS(=O)OH (15%) after the quick rearrangement and dissociation of the secondary ozonide (SOZ) are not negligible.[25] This indicates that measurement of the H_2SO_4 formation may not represent the total amount of tCIs (i.e., the tCI yield from the H_2SO_4 formation measurement accounts for a lower limit). Moreover, when using the method of measuring the H_2SO_4 formation, a high concentration of water (~5500 times higher than the limiting reagent) was required to convert all the produced SO_3 into H_2SO_4, which induced uncertainty in the total capture of tCIs by SO_2 at low pressures, as water is a competitive reactant among the removal pathways of tCIs. It should also be noted that the slope of the increase of the tCI yield in the range of 7-19 Torr in our results is larger than that by Hatakeyama et al.[13] in the same low pressure region. And the slope of the increase in the yield decreases with increasing pressure in the larger pressure range from 10 to 1140 in the results by Hatakeyama et al.[13] (see Figure S5 in SI). This trend was also reported by Hakala et al.[14] in the ozonolysis of 2,3-dimethyl-2-butene. Both suggest that the slope would become significantly smaller at a higher pressure and the nascent yield should be extrapolated from the measurements at low pressures as

close to the zero-pressure limit as possible. Considering all these factors, our method is better suited for the tCI yield measurements at low pressures, especially for the nascent tCI yields.

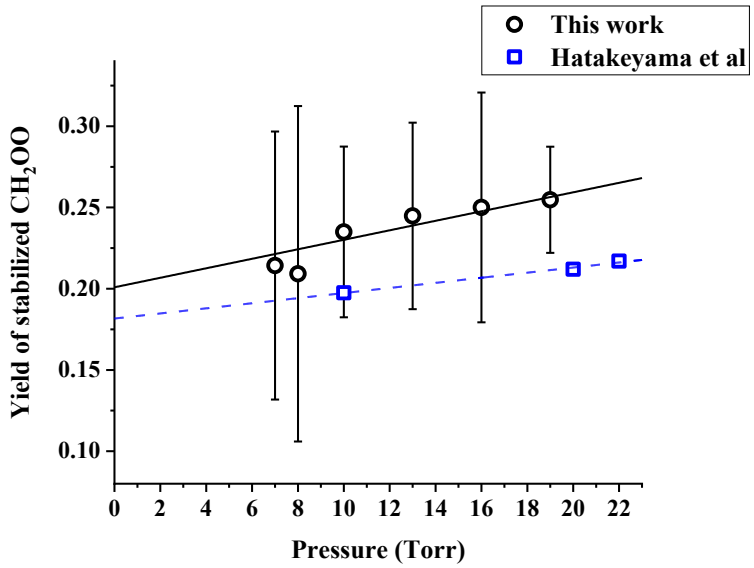

Figure 3. The low-pressure yield of thermalized CH_2OO produced in ozonolysis of ethene measured below 22 Torr. The solid line is the weighted linear fit of the experimental data points and is extrapolated to the zero-pressure limit. The yield measurements from Hatakeyama et al.[13] are included for comparison with the blue line representing the linear fit of their experimental data points below 22 Torr. Error bars represent one standard deviation of repeated measurements at each pressure.

Although the difficulty in making measurements at low pressure limits the experimental studies, the nascent energy distribution and the yield of thermalized CH_2OO produced from ozonolysis of ethene have drawn much attention from theoretical studies. Olzmann et al.[4] reported 20% stabilization of CH_2OO at about 7 Torr using master equation and statistical models, while the more recent calculations by both Pfeifle et al. and Nguyen et al.[26, 27] suggest a higher value of 36% as the nascent tCI yield in ethene ozonolysis. The disagreement between these theoretical works highlights the significance of experimental studies to validate the computational works. Our measurements indicate a nascent tCI yield of 20.1 $\pm$ 2.5% in ethene

ozonolysis, which is close to the value of 20% in the earlier theoretical study by Olzmann et al.[4] but is significantly lower than the value of 36% in the more recent and high-level theoretical studies by Pfeifle et al. and Nguyen et al.[26, 27] This comparison suggests that the internal energy distribution of the nascent tCI might be too low or the isomerization barrier of CH_2OO might be too high in the calculations by Pfeifle et al. and Nguyen et al.[26, 27]

Our experimental value of the nascent tCI yield of 20.1 ± 2.5% is about 22% lower than the IUPAC suggested atmospheric tCI yield in ethene ozonolysis of 42 ± 10 %,[22] showing an obvious pressure dependence of the collisional stabilization of CH_2OO. Hatakeyama et al.[13] also reported a similar increase in the yield by about 18.4% in going from 10 to 760 Torr. However, in the low-pressure region of 7-19 Torr the current work has a larger rate of increase of the tCI yield than that by Hatakeyama et al., although they have about the same zero-pressure tCI yield (Figure S5 in SI). On the other hand, the theoretical works by Olzmann et al., Pfeifle et al., and Nguyen et al. reported that the overall increase of the yield from the zero-pressure limit to atmospheric pressure were1%, 12%, and 12%, respectively,[4, 26, 27] which underestimated the pressure impact on collisional stabilization of the high-energy CH_2OO considering the discrepancies with the experiments in the overall pressure range from 0 to 760 Torr. Further comparison also reveals that the increasing trend in the low-pressure region of 7-19 Torr measured by this work agrees with the theoretical predictions by Nguyen et al.[26] and Pfeifle et al.[27], although the theoretical works reported a higher nascent yield (Figure S5 in SI). The different rates of increase of tCI from the low pressure (faster increase) to the atmospheric pressure (slower increase) indicate pressure-dependent collisional stabilization rate of CIs.

The kinetic modeling is carried out to obtain the pressure-dependent collisional stabilization rate. The unimolecular decomposition and collisional stabilization reactions of high-energy CH_2OO are listed in Table 1. As shown in the theoretical calculation by Nguyen et al.[27],

collisional stabilization of POZ in ozonolysis of ethene is negligible, and the increase of the tCI yield with increasing pressure is due to collisional stabilization of high-energy CIs (reaction (7) in Table 1). The absolute value of the collisional stabilization rate constant of the high-energy CIs used in our modeling is highly dependent on the decomposition rate constant of high-energy CIs. However, only some crude theoretical estimations of this unimolecular decay rate have been reported so far due to the difficulty in measuring the prompt decay of high-energy CIs experimentally.[13, 28, 29] In these theoretical predictions, the overall decomposition rate of the high-energy CIs ($k_2 + k_3 + k_4 + k_6$) has been estimated to be on the order of 10^4 to 10^9 s^{-1}. Thus, the relative collisional deactivation rate $k_7/(k_2 + k_3 + k_4 + k_6)$ of the high-energy CIs is used in the modeling of the pressure-dependent tCI yield. From the low-pressure and nascent yield measurements on tCIs in this work, in combination with the previous results at atmospheric pressure, the deactivation reaction of high-energy CIs to tCIs can be considered as a collisional reaction with buffer gases (reaction (7) in Table 1), and its relative reaction rate under different pressure can be determined by comparing the modeled and experimental tCI yields, as shown in Figure S6 in SI. The value of $k_7/(k_2 + k_3 + k_4 + k_6)$ in ozonolysis of ethene is determined in this work to be 1.5×10^{-19} cm^3 $molecule^{-1}$ below 20 Torr and decrease to 1.7×10^{-20} cm^3 $molecule^{-1}$ at atmospheric pressure.

Table 1. Formation and reactions of high-energy Criegee intermediates. The complete reaction network used to model the ethene ozonolysis system is listed in Table S3 in SI.

(1)	$C_2H_4 + O_3 \rightarrow$ HCHO + 0.201 thermalized CH_2OO + 0.799 High-energy CH_2OO
(2)	High-energy $CH_2OO \rightarrow CO_2 + H_2$
(3)	High-energy $CH_2OO \rightarrow CO + H_2O$
(4)	High-energy $CH_2OO \rightarrow H + HCO_2$
(6)	High-energy $CH_2OO \rightarrow$ HCOOH

(7)	High-energy $CH_2OO + M \rightarrow$ thermalized $CH_2OO + M$

As shown in Figure S7, a comparison of the nascent yield of thermalized CH_2OO to the other tCIs produced from ozonolysis of C4-C6 alkenes (reported in our previous work) indicates that CH_2OO tends to have a higher nascent tCI yield than larger CIs. The nascent yield of thermalized CH_3CHOO produced from cis- and trans-2-butene + O_3 are both below 5%, while the thermalized $C(CH_3)_2OO$ from ozonolysis of 2,3-dimethyl-2-butene has a higher nascent yield of ~12%. Endocyclic tCIs produced from alkenes such as cyclopentene and cyclohexene showed effectively no nascent yield in the low-pressure measurements. Compared to the rest of tCIs, thermalized CH_2OO has a much higher nascent yield of ~20%, agreeing with the relatively high isomerization energy barrier of CH_2OO from theoretical calculations. The energy barriers for the CH_2OO isomerization to form dioxirane and hydroperoxide were reported to be 18.2-19.1 kcal/mol and 30.8-31.8 kcal/mol, respectively, as reported by Olzmann et al. and Nguyen et al.[4, 27] Compared to the 14.8-16.2 kcal/mol and 17.1 kcal/mol isomerization barrier of CH_3CHOO and $C(CH_3)_2OO$ reported by Olzmann et al. and Fang et al.,[4, 30] CH_2OO needs more internal energy to undergo a prompt isomerization or decomposition.

In summary, the yields of thermalized CH_2OO in ethene ozonolysis were determined at low pressures from 7 to 19 Torr by monitoring the consumption of SO_2 scavenger, which allows systematic studies of the nascent yield of tCIs in ozonolysis of various alkenes. The current result from extrapolation to the zero-pressure limit, 20.1 $\pm$ 2.5%, agrees with the previous experimental work at low pressure. However, our experimental nascent yield of tCI is significantly lower than those predicted in the recent calculations by Pfeifle et al. and Nguyen et al.[26, 27] Although the relatively high yield of thermalized CH_2OO compared to large tCIs such as CH_3CHOO and $C(CH_3)_2OO$ validates the theoretical calculation results of a higher isomerization

barrier of CH_2OO, the nascent yield of thermalized CH_2OO reported here indicates that further improvements of the intrinsic reaction dynamics calculations of ethene ozonolysis are needed and provides a benchmark for additional theoretical studies on the energy distribution of CIs produced from ethene ozonolysis. Moreover, while for ethene ozonolysis the value of the yield of thermalized CH_2OO at atmospheric pressure is important, it is mechanistically determined at the molecular level by both the nascent yield of CH_2OO at the zero pressure and the pressure-dependent energy transfer and collisional stabilization rate of CH_2OO from low to atmospheric pressure. This study at the low pressure provides a measurement and shows that the deactivation rate constant of CH_2OO at low pressure < 20 Torr is much higher than that at atmospheric pressure.

Experimental methods. A cylindrical quartz flow cell (length 57 cm, diameter 2.54 cm) was used as a fast reactor for ozonolysis reactions (Figure S1). Ethene was mixed with the N_2 dilution gas and then flowed into the reactor together with O_3 (~1% in O_2) produced by an ozone generator. SO_2 (~4% in N_2) was mixed with alkene before O_3 when tCIs needed to be scavenged for confirmation of tCI identity or tCI yield measurements. The 532 nm output from a Continuum Surelite II Nd: YAG laser pumped a Lambda-Physik dye laser to generate 10 Hz pulse outputs at 640-660 nm using the DCM dye in methanol. An Inrad Autotracker III produced second harmonics in the range of 320-330 nm. A pair of highly reflective mirrors (> 99.9%, Layertec GmbH) centered at 330 nm was used to obtain a baseline ringdown time τ_0 of ~ 5 μs. With a long effective path and high sensitivity ($\alpha_{\min} \sim 3\times10^{-8}$ cm^{-1}), CRDS can capture signals from species at low concentrations.

The average concentration of the targeted species was measured using CRDS according to the following equation:

$$\alpha = \sum_i \sigma_i(\lambda) N_i + f(\lambda) = \frac{L}{c l_s}\left(\frac{1}{\tau} - \frac{1}{\tau_0}\right) \qquad (2)$$

where α is the absorption coefficient, N_i is the number density (molecules per unit volume) of the i-th absorber, σ_i is the absorption cross-section of the i-th species at wavelength λ, c is the speed of light, L is the distance between the two mirrors, l_s is the sample length (distance between the sample input and output), τ is the ring-down time when absorber species are in the cavity, τ_0 is the ring-down time in an empty cavity, and parameter $f(\lambda)$ accounts for the unidentified broad extinction contribution at varying wavelengths.

Supporting Information

The Supporting Information (PDF file) includes more experimental and modeling details. Figures S1-S7 present the experimental setup, the concentration profile of thermalized CH_2OO, measurements on HCHO at low pressure, comparison between theoretical and experimental tCI yields, comparison between modeling and experimental tCI yields, and comparison with other alkene ozonolysis systems. Tables S1-S4 present the previous experimental measurements, flow parameters of the reactor, kinetic modeling, and tCI yields measurements at each pressure.

Author Information

The authors declare no competing financial interests.

Acknowledgement

This work was supported by the US National Science Foundation (CHE-1566636 and CHE-2155232).

References

(1) Paulson, S. E.; Orlando, J. J. The Reactions of Ozone with Alkenes: an Important Source of HOx in the Boundary Layer. *Geophys. Res. Lett.* **1996**, *23*, 3727-3730.

(2) Atkinson, R.; Arey, J. Atmospheric Degradation of Volatile Organic Compounds. *Chem. Rev.* **2003**, *103*, 4605-4638.

(3) Kroll, J. H.; Seinfeld, J. H. Chemistry of Secondary Organic Aerosol: Formation and Evolution of Low-Volatility Organics in the Atmosphere. *Atmos. Environ.* **2008**, *42*, 3593-3624.

(4) Olzmann, M.; Kraka, E.; Cremer, D.; Gutbrod, R.; Andersson, S. Energetics, Kinetics, and Product Distributions of the Reactions of Ozone with Ethene and 2,3-Dimethyl-2-Butene. *J. Phys. Chem. A* **1997**, *101*, 9421-9429.

(5) Osborn, D. L.; Taatjes, C. A. The Physical Chemistry of Criegee Intermediates in the Gas Phase. *Int. Rev. Phys. Chem.* **2015**, *34*, 309-360.

(6) Jr-Min Lin, J.; Chao, W. Structure-Dependent Reactivity of Criegee Intermediates Studied with Spectroscopic Methods. *Chem. Soc. Rev.* **2017**, *46*, 7483-7497.

(7) Welz, O.; Savee, J. D.; Osborn, D. L.; Vasu, S. S.; Percival, C. J.; Shallcross, D. E.; Taatjes, C. A. Direct Kinetic Measurements of Criegee Intermediate (CH_2OO) Formed by Reaction of CH_2I with O_2. *Science* **2012**, *335*, 204-207.

(8) Taatjes, C. A. Criegee Intermediates: What Direct Production and Detection Can Teach Us About Reactions of Carbonyl Oxides. *Annu. Rev. Phys. Chem.* **2017**, *68*, 183-207.

(9) Liu, F.; Beames, J. M.; Petit, A. S.; McCoy, A. B.; Lester, M. I. Infrared-Driven Unimolecular Reaction of CH_3CHOO Criegee Intermediates to OH Radical Products. *Science* **2014**, *345*, 1596-1598.

(10) Taatjes, C. A.; Welz, O.; Eskola, A. J.; Savee, J. D.; Scheer, A. M.; Shallcross, D. E.; Rotavera, B.; Lee, E. P. F.; Dyke, J. M.; Mok, D. K. W.; Osborn, D. L.; Percival, C. J. Direct Measurements of Conformer-Dependent Reactivity of the Criegee Intermediate CH_3CHOO. *Science* **2013**, *340*, 177-180.

(11) Sheps, L. Absolute Ultraviolet Absorption Spectrum of a Criegee Intermediate CH_2OO. *J. Phys. Chem. Lett.* **2013**, *4*, 4201-4205.

(12) Hatakeyama, S.; Kobayashi, H.; Akimoto, H. Gas-Phase Oxidation of SO_2 in the Ozone-Olefin Reactions. *J. Phys. Chem.* **1984**, *88*, 4736-4739.

(13) Hatakeyama, S.; Kobayashi, H.; Lin, Z. Y.; Takagi, H.; Akimoto, H. Mechanism for the Reaction of CH_2OO with SO_2. *J. Phys. Chem.* **1986**, *90*, 4131-4135.

(14) Hakala, J. P.; Donahue, N. M. Pressure-Dependent Criegee Intermediate Stabilization from Alkene Ozonolysis. *J. Phys. Chem. A* **2016**, *120*, 2173-2178.

(15) Berndt, T.; Kaethner, R.; Voigtländer, J.; Stratmann, F.; Pfeifle, M.; Reichle, P.; Sipilä, M.; Kulmala, M.; Olzmann, M. Kinetics of the Unimolecular Reaction of CH_2OO and the Bimolecular Reactions with the Water Monomer, Acetaldehyde and Acetone Under Atmospheric Conditions. *Phys. Chem. Chem. Phys.* **2015**, *17*, 19862-19873.

(16) Newland, M. J.; Nelson, B. S.; Munoz, A.; Rodenas, M.; Vera, T.; Tarrega, J.; Rickard, A. R. Trends in Stabilisation of Criegee Intermediates from Alkene Ozonolysis. *Phys. Chem. Chem. Phys.* **2020**, *22*, 13698-13706.

(17) Newland, M. J.; Rickard, A. R.; Vereecken, L.; Muñoz, A.; Ródenas, M.; Bloss, W. J. Atmospheric Isoprene Ozonolysis: Impacts of Stabilised Criegee Intermediate Reactions with SO_2, H_2O and Dimethyl Sulfide. *Atmos. Chem. Phys.* **2015**, *15*, 9521-9536.

(18) Campos-Pineda, M.; Zhang, J. Low-Pressure Yields of Stabilized Criegee Intermediates CH_3CHOO and $(CH_3)_2COO$ in Ozonolysis of Trans-2-Butene and 2,3-Dimethyl-2-Butene. *Chem. Phys. Lett.* **2017**, *683*, 647-652.

(19) Campos-Pineda, M.; Zhang, J. Product Yields of Stabilized Criegee Intermediates in the Ozonolysis Reactions of Cis-2-Butene, 2-Methyl-2-Butene, Cyclopentene, and Cyclohexene. *Science China Chemistry* **2018**, *61*, 850–856.

(20) Drozd, G. T.; Donahue, N. M. Pressure Dependence of Stabilized Criegee Intermediate Formation from a Sequence of Alkenes. *J. Phys. Chem. A* **2011**, *115*, 4381-4387.

(21) Drozd, G. T.; Kroll, J.; Donahue, N. M. 2,3-Dimethyl-2-butene (TME) Ozonolysis: Pressure Dependence of Stabilized Criegee Intermediates and Evidence of Stabilized Vinyl Hydroperoxides. *J. Phys. Chem. A* **2011**, *115*, 161-166.

(22) Cox, R. A.; Ammann, M.; Crowley, J. N.; Herrmann, H.; Jenkin, M. E.; McNeill, V. F.; Mellouki, A.; Troe, J.; Wallington, T. J. Evaluated Kinetic and Photochemical Data for Atmospheric Chemistry: Volume VII - Criegee Intermediates. *Atmos. Chem. Phys.* **2020**, *20*, 13497-13519.

(23) Keller-Rudek, H.; Moortgat, G. K.; Sander, R.; Sörensen, R. The MPI-Mainz UV/VIS Spectral Atlas of Gaseous Molecules of Atmospheric Interest. *Earth System Science Data* **2013**, *5*, 365-373.

(24) Ianni, J. C. A Comparison of the Bader-Deuflhard and the Cash-Karp Runge-Kutta Integrators for the GRI-MECH 3.0 Model Based on the Chemical Kinetics Code Kintecus. In Computational Fluid and Solid Mechanics 2003; Bathe, K. J., Ed; Elsevier Science Ltd.: Oxford, 2003; pp 1368-1372.

(25) Vereecken, L.; Harder, H.; Novelli, A. The Reaction of Criegee Intermediates with NO, RO_2, and SO_2, and Their Fate in the Atmosphere. *Phys. Chem. Chem. Phys.* **2012**, *14*, 14682-14695.

(26) Pfeifle, M.; Ma, Y. T.; Jasper, A. W.; Harding, L. B.; Hase, W. L.; Klippenstein, S. J. Nascent Energy Distribution of the Criegee Intermediate CH_2OO from Direct Dynamics Calculations of Primary Ozonide Dissociation. *J. Chem. Phys.* **2018**, *148*, 174306.

(27) Nguyen, T. L.; Lee, H.; Matthews, D. A.; McCarthy, M. C.; Stanton, J. F. Stabilization of the Simplest Criegee Intermediate from the Reaction between Ozone and Ethylene: A High-Level Quantum Chemical and Kinetic Analysis of Ozonolysis. *J. Phys. Chem. A* **2015**, *119*, 5524-5533.

(28) Horie, O.; Moortgat, G. K. Decomposition Pathways of the Excited Criegee Intermediates in the Ozonolysis of Simple Alkenes. *Atmos. Environ.* **1991**, *25*, 1881-1896.

(29) Copeland, G.; Ghosh, M. V.; Shallcross, D. E.; Percival, C. J.; Dyke, J. M. A Study of the Ethene-Ozone Reaction with Photoelectron Spectroscopy: Measurement of Product Branching Ratios and Atmospheric Implications. *Phys. Chem. Chem. Phys.* **2011**, *13*, 14839.

(30) Fang, Y.; Liu, F.; Barber, V. P.; Klippenstein, S. J.; McCoy, A. B.; Lester, M. I. Communication: Real Time Observation of Unimolecular Decay of Criegee Intermediates to OH Radical Products. *J. Chem. Phys.* **2016**, *144*, 061102.